Korea-Australia Rheology Journal
Vol. 19, No. 3, November 2007 pp. 109-115

Microchip-based cell aggregometer using stirring-disaggregation mechanism

Sehyun Shin[1]*, Yijie Yang[2] and Jang-Soo Suh[3]
[1]*Department of Mechanical Engineering, Korea University, Seoul, Korea*
[2]*School of Mechanical Engineering, Kyungpook National University, Daegu, Korea*
[3]*Department of Laboratory Medicine, Kyungpook National University Hospital, Daegu, Korea*
(Received July 5, 2007; final revision received August 27, 2007)

Abstract

A new microchip-based aggregometer that uses a stirring-aided disaggregation mechanism in a microchip was developed to measure red blood cell (RBC) aggregation in blood and RBC suspensions. Conventional methods of RBC disaggregation, such as the rotational Couette system, were replaced with a newly designed stirring-induced disaggregation mechanism. Using a stirrer in a microchip, the aggregated RBCs stored in a microchip can be easily disaggregated. With an abrupt halt of the stirring, the backscattered light intensity can be measured in a microchip with respect to time. The time recording of the backscattered light intensity (syllectogram) shows an exponential decreasing curve representing the RBC aggregation. By analyzing the syllectogram, aggregation indices such as *AI* and *M* were determined. The results showed excellent agreement with LORCA. The essential feature of this design is the incorporation of a disposable microchip and the stirring-induced disaggregation mechanism.

Keywords : aggregation, RBC, microchip, aggregometer, stirring

1. Introduction

Red blood cells (RBCs) in normal human blood tend to form linear and branched aggregates. Such aggregation forms face-to-face morphology similar to a stack of coins, which is called rouleaux. Furthermore, RBC aggregation can be reversed, in which case, the RBCs disperse in a high shear environment. The reversible aggregation has a strong correlation with shear-thinning blood viscosity (i.e., the decrease in blood viscosity with the increase in the shear rate due to the dispersion of the aggregates). Since RBC aggregation has been known to be a major determinant of the in vitro rheological properties of blood, it continues to be of interest in the field of hemorheology (Rampling *et al.*, 2004; Stoltz *et al.*, 1999). In sepsis (Baskurt *et al.*, 1997), diabetic mellitus (Bauersachs *et al.*, 1987), myocardial ischemia (Dormandy *et al.*, 1982), and renal failure (Hein *et al.*, 1987), increased RBC aggregation is observed, but the causes of the diseases are different.

Although RBC aggregation is of great importance, there is still a lack of comprehensive understanding. For example, the mechanism that governs this form of cell-cell interaction is not sufficiently known, even the two mechanisms that have been proposed, such as the cross-bridging model and the depletion layer model (Neu *et al.*, 2002). The major cause of aggregation, however, is known to be the presence of large plasma-proteins, especially fibrinogen. Recently, there has been an increasing amount of experimental evidence indicating that RBC cellular properties can markedly affect aggregation. The term "RBC aggregability" describes the cell's intrinsic tendency to aggregate (Rampling *et al.*, 2004). In addition, a question has been raised as to whether hyper-aggregation is really harmful for in-vivo hemodynamics (Meiselman and Baskurt, 2006).

Various techniques for measuring RBC aggregation have been developed (Rampling, 1988). Typical techniques can be briefly summarized as follows: (i) Direct microscopic technique: The most obvious, but labor-intensive and time-consuming approach for quantifying RBC aggregation photographs the diluted blood sample, which is placed between a slide and a cover-slip, and analyzes them by counting the numbers of cellular units that are either a mono-dispersed cell or cellular aggregates (Chien and Jan, 1973); (ii) Electrical impedance technique: Capacitance and resistance of RBC suspensions are measured in a rectangular channel over time (Pribush *et al.*, 1999); and (iii) Light intensity method: This technique is based on the principle of recording the light intensity over time (which is known as a "syllectogram") and analyzing the transient characteristics of the recorded intensity as a measure of RBC aggregation in zero-flow condition. Recording the light intensity either back-scattered (Zhao *et al.*, 1999) from or transmitted (Shvartsman *et al.*, 2001; Shin *et al.*,

*Corresponding author: lexerdshin@korea.ac.kr

2004) through the RBCs under defined shearing conditions has been used to assess different aspects of RBC aggregation. Recently, other techniques including the ultrasound backscattering method (Boynard *et al.*, 1987) have been reported.

Each of these methods allows for the examination of RBC aggregation behavior under zero- or steady-flow conditions. After cells are completely disaggregated by applying a dynamic high-shear flow, they are suddenly exposed to zero-flow condition. Then, the light intensity is recorded over time and the syllectogram is analyzed with a curve-fitting program to determine the aggregation indexes such as the *AI* (aggregation index), half-time ($t_{1/2}$) and *M*-index. For the RBC disaggregation, most of the current techniques, including the commercial aggregometers, adopt a rotational shearing system. In order to obtain a complete disaggregation, a high shear rate above 500 s^{-1} has to be applied. For hyper-aggregated blood samples such as cryoglobulinemia and those with horse blood, however, a much higher shear rate is needed for complete disaggregation. An incomplete disaggregation could cause serious problems in the commercial aggregometer. Thus, the rotational shearing system should be able to generate a high shear rate by increasing the rotational speed. Thus, these rotational shearing systems cause the instruments to be expensive and difficult to design. In addition, they require labor-intensive cleaning after each measurement. Hence, these current techniques, while useful in a research setting, are not optimal for day-to-day clinical use.

Therefore, it is necessary to develop a simple and labor-free instrument that can measure the aggregation indices of RBCs with minimal blood sample. Our recent study (Shin *et al.*, 2005) proposed a vibration-induced disaggregation mechanism with a microchannel, whose implementation for clinical use was found to be very difficult due to vibration-induced noise. Therefore, the objective of the present study is to develop a new aggregometer for use in clinical environment, which should be quick and easy to use and quiet for clinical applications. In the present study, a magnetic stirring-aided disaggregation mechanism was designed for use in a microchip. The rotational stirrer installed in a microchip was remotely rotated by a rotating magnetic mechanism. Thus, this article discusses the operating principles and various phenomena observed throughout the development procedures.

2. Materials and methods

2.1. Sample preparation

Blood was obtained from healthy volunteers who were not on any medications and who provided informed consent. Venous blood samples were drawn from the antecubital vein and collected in Vacutainers (6 ml, BD, Franklin Lakes, NJ, USA) which contained (K2) EDTA as the anti-coagulant. It is noteworthy that this method does not require complicated multi-step processes to prepare blood samples since whole blood can be directly used like other aggregometers. In this study, however, a series of processes were conducted to vary the amount of fibrinogens in blood plasma.

Thus, whole blood was centrifuged at 800×g for 5 min. Plasma and buffy-coat were then removed. To eliminate fibrinogen of the blood samples, RBCs were washed three times with an isotonic phosphate buffered saline (PBS, pH=7.4, 290mOsmol/kg). Using a Gel & Clot Activator containing Vacutainers (BD, Franklin Lakes, NJ), serum was obtained. After incubating the serum at 37°C for 1 hour, fibrinogen was added into the serum and mixed well using a vortex stirrer. Then, the washed RBCs were resuspended in a fibrinogen-added serum with fixed hematocrits at 45%. There was no hemolytic presence during the entire test and all analyses were completed within two hours after the collection of blood.

2.2. Apparatus and operational procedure

The schematic of the microchip-based cell aggregometer system is shown in Fig. 1. This system consisted of three sub-systems: 1) Microchip-stirring system; 2) Laser backscattering system (Optical detection system); and 3) Data analyses system. The microchip-stirring system consists of a magnetic rotation mechanism and a microchip including a stirring bar. The magnet-rotation mechanism consists of a rectangular magnet, a rotor, a motor and stirrer in a microchip. As the magnet mounted on the rotor rotates, the stirrer in the microchip rotates. The rotating speed, which can be controlled by the input voltage of the motor, was varied from 100 to 5,000 rpm. To stop the rotating magnet abruptly, a mechanical brake is applied on the axis of the rotor. The laser backscattering system consists of a diode laser (650 nm) and a photodiode, which is of very good sensitivity (0.9) at 650 nm. Backscattered light detected by the photodiode are converted to digital signals by the DAQ card (NI, USA) and transferred to a computer. Then, the signals are analyzed by the Labview program (data analyses system) to obtain the indices of RBC aggregation.

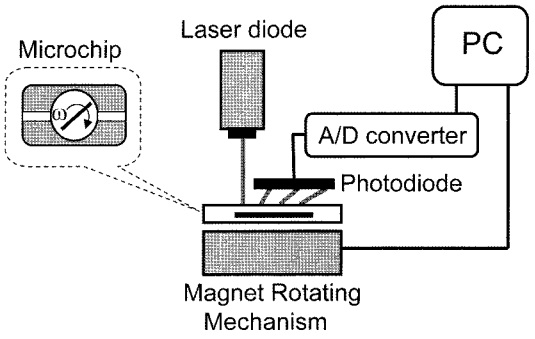

Fig. 1. Schematic diagram of the apparatus.

The essential feature of the present aggregometer is the use of a stirring mechanism to disaggregate the RBC aggregates. As the magnet is rotated by the motor, the stirrer also is rotated, and the RBCs in the microchip are disaggregated within a short period of time. Another essential feature of the present aggregometer is the use of a disposable microchip, which was designed to plug-in and -out of the test instrument. The disposable microchip was made of plastic or glass.

The procedures of the typical tests that were conducted were as follows: The test fluid is placed in the chamber of a microchip, which has a stirrer inside, and the inlet and outlet of the microchip are sealed with a sealant. Then, the microchip is mechanically mounted onto the jig, which is 10 mm apart from the magnetic rotating mechanism. In order to disaggregate the RBC aggregates, a defined stirring was applied for 10~20 *s* and then stopped abruptly. Of course, even after the sudden stop of the rotational mechanism in the present system, there was a transitional phase from a high shear rate, rapidly decreasing to zero. However, the transition duration, which may depend on the plasma viscosity and aggregometer geometry, was reported to be much shorter (<0.2 s) than the whole syllectogram period (~120 s) (Chien and Jan, 1973).

Then, the laser light emitted from the laser diode irradiates the blood sample and part of light is backscattered from the blood sample. The backscattered light is detected by the photodiode, which is linked to the data acquisition system by a computer. When the stirring is stopped suddenly, the disaggregated RBCs start to aggregate. The light intensity is recorded over time in a syllectogram, as shown in Fig. 2. The more the aggregation occurs, the more the light transmits and the less the backscattered light becomes. In the syllectogram after sudden cessation of stirring, the conventional mathematical representation of the syllectogram adopts the bi-exponential representation as shown in Eq. (1):

$$I(t)=I_f \cdot e^{-t/T_f}+I_s \cdot e^{-t/T_s}+I_0 \quad (1)$$

where T_f and T_s denote the time constants of the aggregation process. In fact, aggregation can be considered a multi step process (i.e doublet-, rouleaux-, 3D-aggregate formation), which only takes minutes. However, T_f and T_s in the bi-exponential equation represent the time constants of fast rouleaux formation and slow three-dimensional aggregate formation, respectively.

At time $t=0$, the maximum intensity is obtained, $I_{(t=0)}=I_{max}$. The parameters of aggregation as measures of the RBC aggregation are determined from the syllectogram using a curve-fitting program shown in Fig. 2. These parameters of aggregation are well defined in a previous study (Hardeman *et al.*, 1994) as follows:

(1) *Amplitude (Amp)*: The difference between the maximum light intensity and the light intensity at 120s ($I_{max}-I_0$), indicating the extent of RBC aggregation.

(2) *Half time ($t_{1/2}$)*: The time required to reach a light intensity of "minimum intensity + 1/2 Amp", indicating the characteristic time constant to reach the half level of aggregation. This may be regarded as the exponent of the single exponential curve-fitted equation.

(3) *M-index*: The area above the syllectogram over a 10 s time period (A), indicating degree of the accumulated aggregation during 10 s.

(4) *Aggregation Index (AI)*: The ratio of the area above syllectogram (A) to the total area (A+B) over a 10 s time period, indicating the normalized degree of accumulated aggregation.

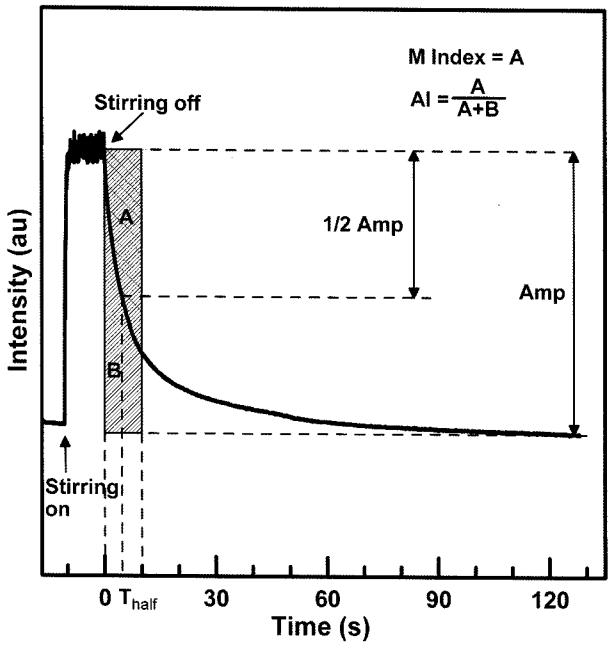

Fig. 2. Syllectogram and aggregation indices.

3. Results and discussion

3.1. Optimization of system and operation

As shown in Fig. 3, the microchip consists of a test chamber, two inlets, and a stirrer. Transparent glass was used for top and bottom of the microchip and a double-sided adhesive tape was multi-stacked on the bottom glass. By removing the part of the adhesive tape using a specialized tool, specified shapes of inlets and the test chamber were made. Then, the top glass was placed on the shaped adhesive tape, and the side walls were fixed with epoxy to fix the gap. Throughout our preliminary study, it was found that there were optimal operating conditions that yielded the same results as the commercial instruments. The optimization was strongly dependent on the relative dimensions of the microchip and stirrer. Thus, the present study investigated the effects of two ratios: the ratio of stirrer diameter to chamber height (d/H) and the ratio of stirrer

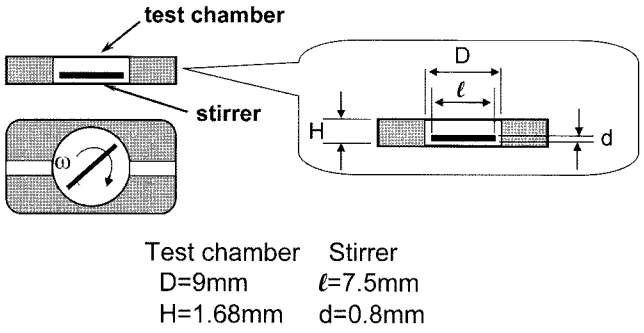

Fig. 3. Dimensions of a microchip.

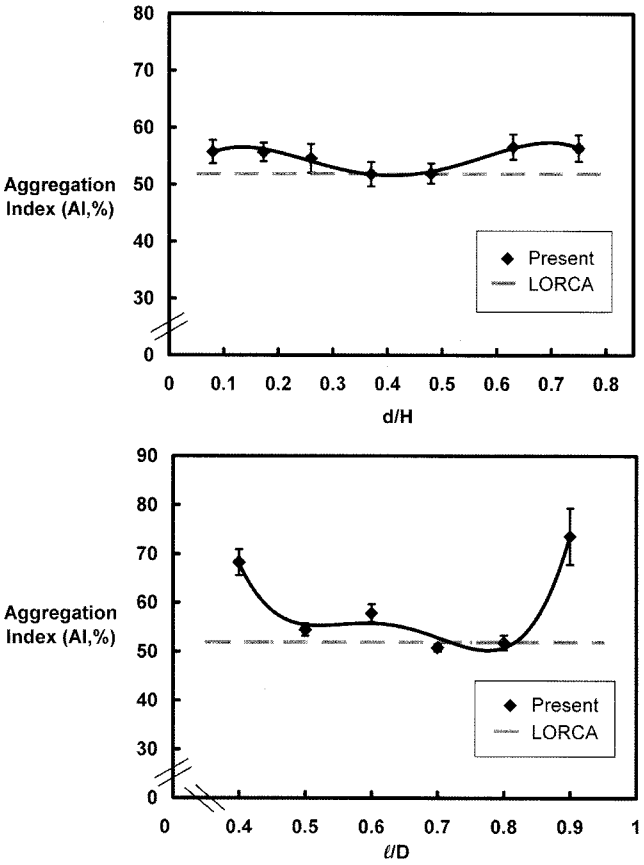

Fig. 4. Effects of dimension of microchip (d/H, *l*/D) on aggregation index.

length to chamber diameter (*l*/D).

Fig. 4 shows the effects of the two ratios on the aggregation index. The present aggregation index *AI*, measured with varying d/H and *l*/D, was compared with that of a commercial aggregometer, LORCA (R&R Mechatronics, Netherlands) at fixed rotating speed (ω=1,000 rpm). As shown in Fig. 4, at the intermediate range of these ratios, the present measurements show good agreement with LORCA results, which were taken as reference. The optimal ratio of d/H is 0.25~0.5 in Fig. 4. In other words, either stirrer diameter or chamber height can be determined relatively considering each other. Except for extremely low

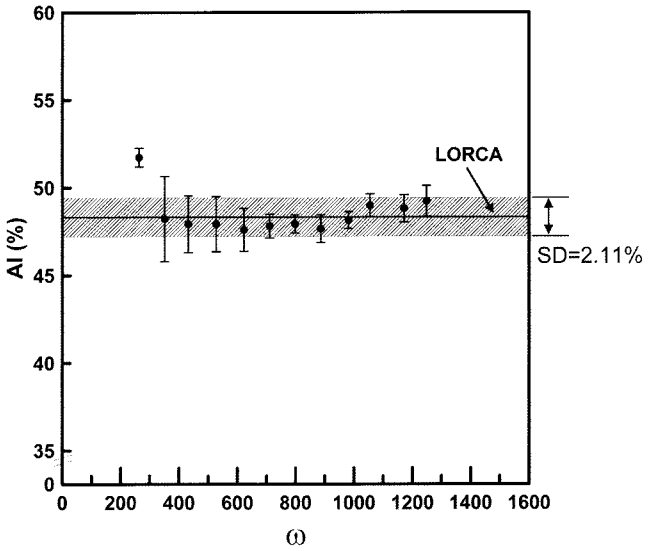

Fig. 5. Effect of rotational speed of stirrer on aggregation index (AI).

or high ratio of d/H, the present AI values are within 2% deviation from the reference. Furthermore, for the ratio of *l*/D, the optimal range is 0.65~0.85 in Fig. 4. Except for an extremely low or high ratio of *l*/D, the present values of AI are also within 2% deviation from the reference. This fact implies that the stirring-induced disaggregation is quite effective in moderate dimensions of a microchip. Considering the deviation and repeatability, the optimal values for the two ratios were determined as d/H=0.47 and *l*/D = 0.83, respectively. In the present study, the diameter and height of the test chamber were 9 mm and 1.68 mm, whereas the length and diameter of the stirrer were 7.5 mm and 0.8 mm respectively. The Volume of blood sample required for one test was 120 μl.

Fig. 5 shows the effect of rotation speed of stirrer on the aggregation index. The rotational speed of the stirrer was measured by the principle of optical tachometer, and the rotating speed was controlled by varying the input voltage of the motor. At each speed, measurements were done five times with the same blood sample. In Fig. 5, the solid line is the AI result from LORCA, and the hatched area means standard deviation (SD) of LORCA. As the figure shows, when the speed of the stirrer is down to less than 710 rpm, the AI values show relatively large SD, and when the speed decreases to 300 rpm, the AI value largely deviates from the reference AI value. This is due to the incomplete RBC disaggregation from weak stirring. As discussed above, the stirring-induced disaggregation was effective in a microchip, so all measured AI values were within the standard deviation of LORCA (2.1%) except for extremely low rotational speeds. Despite of the effective disaggregation for a wide range of stirring speed, the optimal rotational speed should be carefully chosen. For instance, a hyper-aggregated blood sample requires high stirring speed

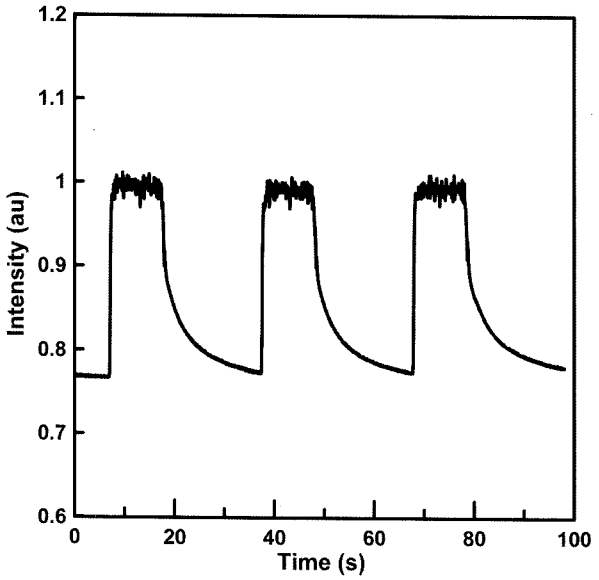

Fig. 6. Kinetics of RBC aggregation and disaggregation.

but such speed may cause hemolysis of RBCs. In the present study, the rotational speed of the stirrer was fixed at 1054 rpm at a fixed input voltage of the motor (8 V).

3.2. Effect of cell age and fibrinogen

Fig. 6 shows the syllectogram of RBC aggregation and disaggregation obtained from the present apparatus. The output signal of the photodiode, which is proportional to the intensity of the backscattered light, is plotted as a function of time. As the stirrer started to rotate, the plateau value was immediately reached within a few seconds. Due to the rotating stirrer, the signal somewhat fluctuated at the plateau. After the abrupt cessation of stirring, the backscattered light exponentially decreased. Whenever the stirring restarted, the same plateau value was reached. This fact implies that several repeated tests can be done with a single microchip.

Good reproducibility was obtained from 10 repeated measurements on the aliquots of the same blood sample. The mean, standard deviation (SD) and CV of various aggregation parameters are shown in Table 1. The most reproducible index was the AI, with a CV of 0.99%. The *M*-index, half time and Amp index also showed high reproducibility with low CV values (less than 2.82%). Other repeated measurements of the different aggregation indices on different samples yielded a similar pattern of precision. In addition, Table 1 compares the values for the RBC aggregation indices measured by the present aggregometer and a commercial aggregometer (LORCA). The test results between the two instruments showed a strong correlation with less than 3.0% relative variation (RV).

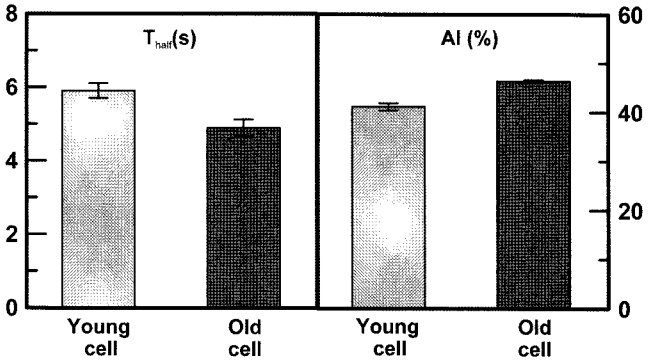

Fig. 7. Comparison of aggregation indices for young and old cells suspended in autologous plasma.

Fig. 7 shows the effect of cell density on RBC-aggregation by comparison of the two aggregation indices of young and old cells suspended in autologous plasma. In fact, cell density is directly related with cell age. In other words, the older the cells, the higher the density of red cells. Thus, through high speed centrifugation (15,000 rpm for 20 min), a density-based separation can be achieved. As shown in Fig. 7, the young cells have a longer half time constant and a smaller AI than the old cells. The detailed RBC-aggregation indices are summarized in Table 2 for the young and old cells. The M-index, Amp and AI of the old cell suspension increased significantly, by 41.26%, 25.41% and 17.70% from those of the young cell suspension, respectively. Also, the half time of the old cell suspension decreased significantly, by 17.17% from that of the young cell suspension. These results indicate that the old cells have higher aggregability than the young cells and that the present instrument can differentiate this cell age effect on RBC aggregation.

Aggregation index was also examined by using various

Table 1. Comparison of RBC aggregation indices measured by the present and LORCA aggregometers

	Present Aggregometer		LORCA		
	Mean±S.D.	CV (%)	Mean±S.D.	CV (%)	RV (%)
AI (%)	48.1±0.5	0.99	48.3±2.0	2.11	−0.38
Amp (au)	20.9±0.4	1.69	20.4±1.4	6.77	2.49
M (au·s)	100.5±1.6	1.60	98.3±5.1	5.23	2.20
$T_{1/2}$ (s)	4.31±0.12	2.82	4.32±0.19	4.37	−0.32

Table 2. Aggregation indices and percentage difference for young and old cells suspended in autologous plasma

Aggregation Indexes	Young	Old	Percentage Difference
AMP (au)	19.1	23.9	25.41 (%) ↑
$T_{1/2}$ (s)	5.91	4.89	−17.17 (%) ↓
M Index	78.6	111.0	41.26 (%) ↑
AI (%)	41.2	46.4	12.70 (%) ↑

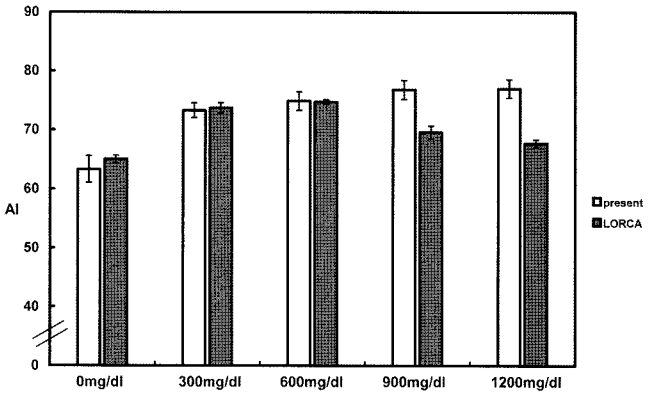

Fig. 8. Relation of fibrinogen concentration and RBC aggregation index measured by present aggregometer and LORCA.

Table 3. Values of aggregation index vs. fibrinogen concentration in blood sample measured by the present aggregometer and LORCA

Fibrinogen Level (mg/dl)	Present Aggregometer		LORCA	
	Mean AI±S.D.	CV (%)	Mean AI±S.D.	CV (%)
0	63.3±2.3	3.56	65.0±0.6	0.98
300	73.3±1.2	1.69	73.7±0.9	1.16
600	74.8±1.6	2.11	74.7±0.4	0.52
900	76.8±1.6	2.12	69.6±1.1	1.56
1200	77.0±1.6	2.03	67.7±0.7	0.97

blood samples, which were modulated by the amount of fibrinogen in blood plasma (Fig. 8 and Table 3). Five different RBC suspensions (45% hematocrits) were prepared by varying the fibrinogen concentration (0, 300, 600, 900, and 1200 mg/dL) in serum. A normal range of fibrinogen in human blood is between 150 and 300 mg/dL. Analyzing all the samples, there was a significant relationship between plasma fibrinogen and AI measured by the present aggregometer. AI showed a strong dependence of fibrinogen for all concentrations. The higher the concentration of fibrinogen in the serum, the higher the aggregation of RBCs; this meant a higher AI even for hyperaggregation induced by fibrinogen. Fig. 8 and Table 3 show the strong correlation between two instruments when fibrinogen concentration is up to 600 mg/dl. However, beyond 900 mg/dl, AI measured by LORCA does not show further increase, whereas the present measurement does. The lower AI value of LORCA may be due to incomplete disaggregation at initial high shear flow, whose shear rate is normally set at 500 s^{-1}.

This may be solved by increasing the initial shear rate for hyper-aggregated blood sample. However these results demonstrated that the present stirring mechanism in a microchip provided sufficiently strong disaggregation even for hyper-aggregated blood sample. Considering the rotational speed of stirrer and the dimensions of the present microchip, the average and maximum shear rates are approximately 800 and 3200 1/s, respectively. Since these shear rates are much larger than that of LORCA, the present system can disaggregate the hyper-aggregated blood sample as shown in Fig. 8. However, such high shear rates in the test chamber could cause mechanical damages on cell membrane, which may be followed by hemolysis of cells. Thus, the operation time of stirrer and its rotational speed should be carefully determined to avoid any possible hemolysis. However, there was any hemolysis observed in the present study.

4. Conclusions

The present study described a newly developed microchip-based aggregometer, which integrated an optical detection method, disposable microchip, and magnetic stirring-induced disaggregation mechanism. Rotating Couette system used by common commercial aggregometers was successfully replaced with a microchip-stirring mechanism. Even though the present study required relatively large quantity of blood sample, the present study, as a proof-of-principles, provided the optimal conditions for stirring-based microchip aggregometer, which can be significantly minimized and require extremely small amount of blood sample. Additionally, the present study demonstrated that the results which were taken with the proposed aggregometer showed excellent agreement with those of a representative commercial aggregometer (LORCA). Conclusively, the present study demonstrated the novel features of the present microchip-based cell aggregometer, which can be used in a clinical setting.

Acknowledgements

This work was supported by Grants from the MOST/KOSEF to the National Core Research Center for Systems Bio-Dynamics (R15-2004-033) and the National Research Laboratory for Biorheology (No: ROA-2003-000-10306-0).

References

Baskurt, O.K., A. Temiz and H.J. Meiselman, 1997, Red blood cell aggregation in experimental sepsis, *J. Lab. Clin. Med.* **130**, 183-190.

Bauersachs, R.M., S. Shaw, A. Zeidler and H.J. Meiselman, 1987, Hemorheological finding in uncontrolled type II diabetes mellitus, *Clin. Hemorheol.* **7**, 432-437.

Boynard, M., J.C. Lelievre and R. Guillet, 1987, Aggregation of red blood cells studied by ultrasound back-scattering phenomenon, *Biorheology* **24**, 451-461.

Chien, S. and K.M. Jan, 1973, Ultrastructural basis of the mechanism of the rouleaux formation, *Microvas. Res.* **5**, 155-166.

Dormandy, L., E. Ernst, A. Matrai and P.T. Flute, 1982, Hemorheologic changes following acute myocardial infarction, *Am. Heart J.* **104**, 1364-1367.

Hardeman, M.R., P.T. Goedhart, J.G.G. Dobbe and K.P. Lettinga, 1994, Laser-assisted optical rotational cell analyzer (L.O.R.C.A): A new instrument for measurement of various structural hemorheological parameters, *Clinical Hemorheology* **14**, 605-618.

Hein, H.J., R.M. Bauersachs, E.I. Feinstein and H.J. Meiselman, 1987, Hemorheological abnormalities in chronic renal failure patients, *Clin. Hemorheol.* **7**, 425-431.

Meiselman, H.J. and O.K. Baskurt, 2006, Hemorheology and hemodynamic: Dove andare?, *Clinical Hemorheol. And Microcirc.* **35**, 37-43.

Neu, B. and H.J. Meiselman, 2002, Depletion-mediated red blood cell aggregation in polymer solutions, *Biophys. J.* **83**, 2482-2490.

Pribush, A., H.J. Meiselman, D. Meyerstein and N. Meyerstein, 1999, Dielectric approach to the investigation of erythrocyte aggregation: I. Experimental basis of the method, *Biorheology* **36**, 411-423.

Rampling, M.W., 1988, Red cell aggregation and yield stress, in *Clinical Blood Rheology* Vol. edited by G.D. Lowe, CRC Press, Boca Raton, Florida, USA, 46-64.

Rampling, M.W., H.J. Meiselman, B. Neu and O.K. Baskurt, 2004, Influence of cell-specific factors on red blood cell aggregation, *Biorheology* **41**, 91-112.

Shvartsman, L.D. and I. Fine, 2001, Light scattering changes caused by RBC aggregation: physical basis for new approach to non-invasive blood count, *SPIE proc.* **4263**, 131-142.

Shin, S., M.S. Park, J.H. Jang, Y.H. Ku and J.S. Suh, 2004, Measurement of red blood cell aggregation by analysis of light transmission in a pressure-driven slit flow system, *Korea-Australia Rheology Journal* **16**, 129-134.

Shin, S., J.H. Jang, M.S. Park, Y.H. Ku and J.S. Suh, 2005, A noble RBC aggregometer with vibration-induced disaggregation mechanism, *Korea-Australia Rheology Journal* **17**, 9-13.

Stoltz, J.F., M. Singh and P. Riha, 1999, *Hemorheology in Practice*. IOS Press, Amsterdam.

Zhao, H., X. Wang and J.F. Stolz, 1999, Comparison of three optical methods to study erythrocyte aggregation, *Clinical Hemorheol. And Microcirc.* **21**, 297-302.